Continued warming could transform Greater Yellowstone fire regimes by mid-21st century

Anthony L. Westerling[a,1], Monica G. Turner[b,1], Erica A. H. Smithwick[c], William H. Romme[d], and Michael G. Ryan[e]

[a]Sierra Nevada Research Institute, University of California, Merced, CA 95343; [b]Department of Zoology, University of Wisconsin, Madison, WI 53706; [c]Department of Geography and Intercollege Graduate Degree Program in Ecology, Pennsylvania State University, University Park, PA 16802; [d]Warner College of Natural Resources, Colorado State University, Fort Collins, CO 80523; and [e]US Department of Agriculture Forest Service, Rocky Mountain Research Station, Fort Collins, CO 80526

Contributed by Monica G. Turner, June 24, 2011 (sent for review May 28, 2011)

Climate change is likely to alter wildfire regimes, but the magnitude and timing of potential climate-driven changes in regional fire regimes are not well understood. We considered how the occurrence, size, and spatial location of large fires might respond to climate projections in the Greater Yellowstone ecosystem (GYE) (Wyoming), a large wildland ecosystem dominated by conifer forests and characterized by infrequent, high-severity fire. We developed a suite of statistical models that related monthly climate data (1972–1999) to the occurrence and size of fires >200 ha in the northern Rocky Mountains; these models were cross-validated and then used with downscaled (~12 km × 12 km) climate projections from three global climate models to predict fire occurrence and area burned in the GYE through 2099. All models predicted substantial increases in fire by midcentury, with fire rotation (the time to burn an area equal to the landscape area) reduced to <30 y from the historical 100–300 y for most of the GYE. Years without large fires were common historically but are expected to become rare as annual area burned and the frequency of regionally synchronous fires increase. Our findings suggest a shift to novel fire–climate–vegetation relationships in Greater Yellowstone by midcentury because fire frequency and extent would be inconsistent with persistence of the current suite of conifer species. The predicted new fire regime would transform the flora, fauna, and ecosystem processes in this landscape and may indicate similar changes for other subalpine forests.

Fire structures ecological systems across multiple scales and is an important component of the Earth system (1, 2). High-severity fire is characteristic of boreal and subalpine forests, including extensive conifer forests of western North America (3–6). High-severity fires are generally large, infrequent (i.e., fire return intervals are often 100–300 y), stand replacing, and driven by climatic effects on fuel flammability rather than by fuel quantity (5, 7–9). Fewer than 5% of fires account for >95% of area burned (3, 10). High-severity fires kill trees and initiate secondary succession, shifting stand age and structure and driving subsequent carbon storage, habitat patterns, and fuel loadings. Improved knowledge of fire dynamics is key to understanding Earth's coupled climate–carbon system (e.g., refs. 11–14). For residents and land managers of fire-prone regions, potential changes in fire dynamics have vast implications for vulnerability of future ecosystem services.

Fire regimes are shifting, and the tempo of change appears to be accelerating. With the warming of Earth's climate (15), fire frequency, extent, severity, and seasonality are expected to change profoundly in the future, with substantial increases in fire activity in many areas (9, 16–21). In the presence of a gradually changing driver such as climate, fire is a fast variable that triggers rapid and significant ecological change. However, there is substantial regional variation in climate–fire relationships (e.g., refs. 2 and 22–24), and a key challenge is translating broad-scale future fire predictions to scales relevant for anticipating ecological consequences and managing natural resources. Of central importance are the magnitude of anticipated changes in fire (e.g., annual area burned and fire return interval) and whether rapid changes may occur soon (14, 18).

Ecosystem resilience may be compromised by novel disturbance regimes (9, 25, 26), and fire regimes may be sensitive indicators of tipping elements (*sensu* ref. 27) that exhibit threshold-like behavior and qualitatively change regional ecosystems. Lenton et al. (27) define tipping elements as subsystems that can be switched into qualitatively different states by small perturbations. The tipping point is the corresponding critical point—in forcing—beyond which the system is qualitatively altered. For example, successive fires in a relatively short time (i.e., compound disturbances) (25) may have synergistic effects, and thus the increased temperatures that drive more frequent fires could constitute a tipping point. Whether increased disturbance frequency will produce qualitative ecosystem changes will depend on the degree to which a community has recovered from the first disturbance when affected by a second. In fire-resilient plant communities, postfire successional trajectories typically lead to vegetation similar to the prefire community (28). Sequential fires could convert such forests to other plant communities if the interval between fires is less than that required to ensure postfire tree regeneration (e.g., to develop the canopy seedbank stored in serotinous cones that allows some conifer species to reestablish after high-severity fire) (29, 30).

Recent evidence suggests that forests in the northern Rocky Mountains are close to a temperature threshold for fire vulnerability (29, 31). The Intermountain West is relatively arid, but dense conifer forests occur at higher elevations and more northerly latitudes where cool temperatures and snow-dominated precipitation support tree growth. Canopy fuels necessary to carry large fires are plentiful, but fuel flammability is controlled by climate. Throughout the West, forest area burned is most strongly associated with low precipitation, low moisture indexes (e.g., moisture deficit, Palmer drought severity) and high temperatures; numerous studies suggest that temperature and its effects on moisture are the most important controls on large fire occurrence and extent (e.g., refs. 18 and 32). Fire suppression, exclusion, and fuel treatment influences are detectable to varying degrees across forest types, but of secondary importance in most forests, especially at higher elevations (24, 33). Large fires have increased in the northern Rockies in recent decades in association with warmer temperatures, earlier snowmelt, and longer fire seasons (31). Midelevation Rocky Mountain forests with stand-replacing fire regimes have been most sensitive to climate warming, accounting for approximately two-thirds of recent west-wide increases in large forest fires (31). This change corresponds to increased spring

Author contributions: A.L.W., M.G.T., E.A.H.S., W.H.R., and M.G.R. designed research; A.L.W. performed research; A.L.W. analyzed data; and A.L.W. and M.G.T. wrote the paper.

The authors declare no conflict of interest.

Freely available online through the PNAS open access option.

[1]To whom correspondence should be addressed. E-mail: turnermg@wisc.edu.

This article contains supporting information online at www.pnas.org/lookup/suppl/doi:10.1073/pnas.1110199108/-/DCSupplemental.

and summer temperatures of <1 °C and earlier spring snowmelt across a large area. However, what this portends for the timing and magnitude of future climate-driven changes in fire is not well understood.

Here we consider how the occurrence, size, and spatial location of large fires (>200 ha) in the Greater Yellowstone ecosystem (GYE) (Fig. S1) might change with climate change. The GYE is one of the most pristine and well-studied wildland ecosystems of temperate North America and an ideal natural laboratory for exploring climate–fire relationships. Fire return intervals of 100–300 y have characterized GYE forests for the past 10,000 y (34), and intervals of 75–100 y were documented in lower elevation forest–steppe vegetation (35, 36). We developed and cross-validated unique statistical models relating observed northern Rockies fires to land-surface characteristics, observed 1972–1999 climate, and hydrology simulated with the variable infiltration capacity (VIC) hydrologic model (37). We combined a logistic regression model to predict the probability of fire (>200 ha) occurrence with a Poisson lognormal model to predict the number of fires given at least one occurred and a generalized Pareto distribution (GPD) model to predict fire size. The statistical models were then used with monthly output from three downscaled (~12 km × 12 km grid) global climate models (GCMs) and VIC to simulate 1,000 monthly fire occurrence and area burned histories for each scenario for the GYE through 2099 and to calculate expected fire rotations—the time to burn an area equal to the area of a landscape of interest (10). See *Methods* and *SI Text* for further details.

We used climate scenarios (Fig. S2) from three GCMs [National Center for Atmospheric Research (NCAR) CCSM 3.0, Centre National de Recherches Météorologiques (CNRM) CM 3.0, and Geophysical Fluid Dynamics Laboratory (GFDL) CM 2.1] from the Intergovernmental Panel on Climate Change (IPCC)'s Fourth Assessment ("AR4") (14), forced with a medium-high emissions pathway (Special Report on Emissions Scenarios "SRES A2") (38). These three GCMs are among a subset of AR4 models suitable for the western United States because of their depiction of seasonal variations in temperature and precipitation and multiyear variability in Pacific sea-surface temperature on the scale of El Nino/Southern Oscillation (39, 40). The A2 emissions scenario was selected as reasonably consistent with trends over recent decades in anthropogenic carbon emissions (41). Future emissions of greenhouse gases and their short-term feedbacks to climate are uncertain. However, most scenarios do not begin to differ meaningfully until midcentury, and our results for the next several decades should be somewhat robust to the choice of emissions scenario.

Our approach assumes that the fundamental relationships between climate and fire are stationary, but changes in the frequency and location of climatic conditions conducive to large fires will influence fire activity. Because this stationarity assumption will be violated once climate shifts beyond the conditions that sustain the current ecosystem and fire regime, our approach is most useful for determining responses to climate change in the coming decades and identifying when the climate–fire–vegetation system might not be sustained in its present form.

Results

Our combined statistical models predicted fire and characterized extreme fire years in the Northern Rockies more effectively than has been done previously (Fig. 1 and *SI Text*). Temperature, precipitation, and moisture deficit were all important for predicting fire occurrence and number; given that a fire occurred, cumulative water year moisture deficit was key for estimating fire size distributions (*SI Text*). The models explained 83% of interannual variation in large fire occurrence and 73% of the variation in burned area for the calibration dataset. For the model estimation period in the Northern Rockies, 33% of fires

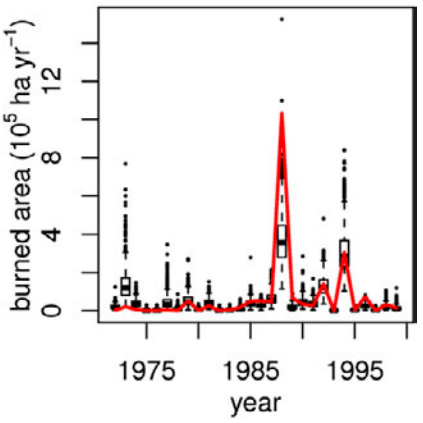

Fig. 1. Annual area burned by large fires in the Northern Rockies: observed (*line*) versus predicted from 1,000 simulations per month, aggregated across 2,309 grid cells (boxes show interquartile range; whiskers, 1.5× interquartile range; and points, extremes). Results are a composite of simulations for fire presence/absence using probabilities from cross-validated logistic regressions, simulations for fire size from cross-validated Poisson lognormal distributions conditional on fire presence and the linear estimator from the cross-validated linear regression, and fire size estimated using a generalized Pareto distribution conditional on fire occurrence and moisture deficit (see also Figs. S6–S9). The generalized Pareto is validated elsewhere (*SI Text* and Figs. S7 and S8).

and 66% of burned area occurred during the two largest fire years (1988 and 1994); 30% of fires and 45% of burned area in our simulation also occurred during those two years (*SI Text* and Fig. S3). High fire activity always occurred during warmer-than-average years, and this pattern was clear within the GYE (Fig. S4). The relationship between temperature and fire was nonlinear, and only ~0.5 °C above the 1961–1990 average spring and summer temperature (March–August) distinguished large-fire years from most other years in the GYE (Fig. S4). Warmer-than-average temperatures were a necessary but not sufficient condition for predicting extreme fire years; in addition to temperature, moisture deficit and summer precipitation (July–August) also influenced fire during warm years (Fig. S6). Our methods captured broad-scale topographic variability in climate (e.g., cooler temperatures at higher elevations), which is necessary for regional fire projections. The probabilistic models enabled robust estimates of fire response to changing climate, including extreme fire years, by running large numbers of simulations (*SI Text*).

Fire simulations for three downscaled GCM scenarios for the recent historical period (1950–1990) in the GYE produced realistic interannual variation in area burned and no directional trends (Fig. 2). Predicted area burned was <10,000 ha (<1.25% of the GYE) in most years and agreed well with observed variability; however, no simulated fire years were as extreme as 1988 before the first decade of the 21st Century. This result is not unexpected; 1988-scale events in the GYE are necessarily very rare (otherwise historical fire rotations would be less than the observed >120 y). In addition, our hydrologic simulations cannot incorporate extremes in day-to-day variability in wind speed because downscaled wind fields are not yet available. Because extreme dry conditions in the recent historical record resulted from climate (high temperature and low precipitation) and weather (high winds), the simulated dry extremes in moisture deficit using climatological winds are likely underestimated.

Post-1990 simulations projected substantial increases in GYE fire (Fig. 2). Notably, by 2020 projected increases in burned area over a 1951–1990 reference period were detectable with 95% confidence over 100% of simulations using one-sided Mann–

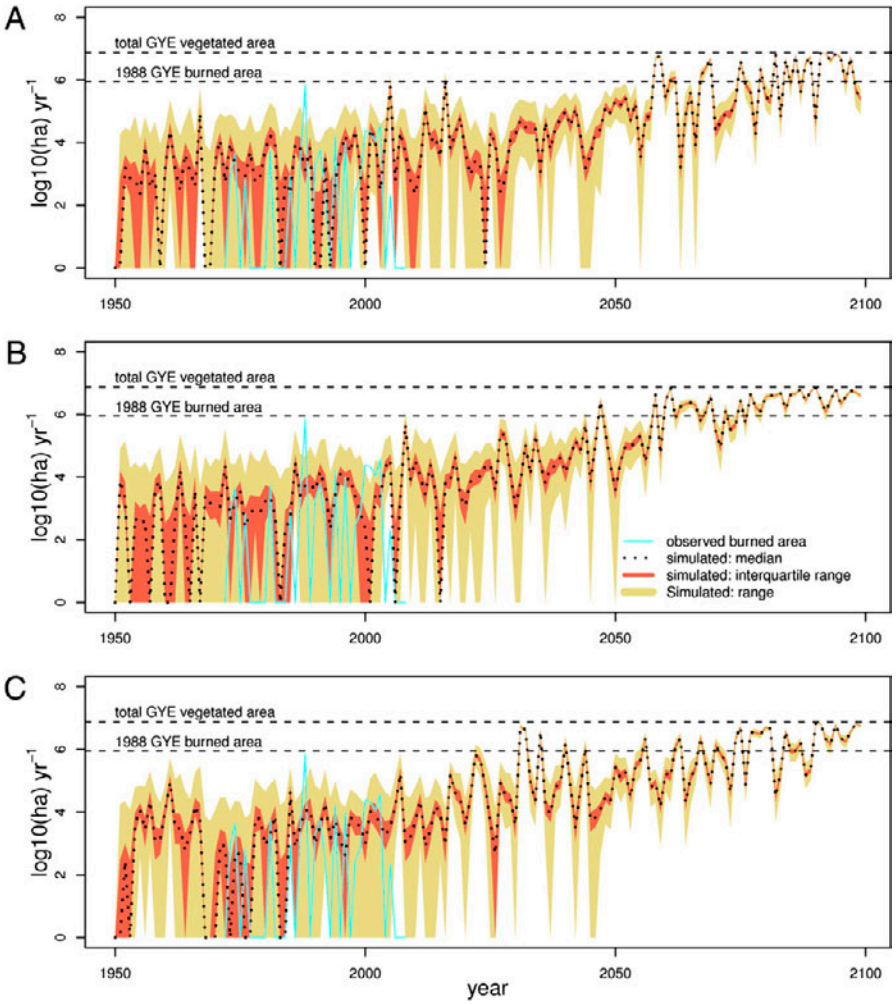

Fig. 2. The range (light shading), interquartile range (dark shading), and median (dotted line) of predicted area burned for 1,000 gridded monthly simulations, aggregated over the GYE by year, and the observed annual area burned (solid line) for three downscaled GCM SRES A2 climate scenarios: NCAR CCSM 3.0 (*A*), CNRM CM 3.0 (*B*), and GFDL CM 2.1 (*C*).

Whitney tests. Fire seasons comparable to 1988 became more frequent, with between one (for NCAR) and five (for GFDL) such events occurring between 2011 and 2050. After 2050, all models predicted that annual area burned would exceed 100,000 ha during most years. Years with no large fires—common in the historical record—became extremely rare by 2050 and did not occur in 1,000 simulations after 2050 for either the CNRM or GFDL scenarios and occurred only three times in the 1,000 NCAR simulations. This increase in average annual "background" area burned in years without 1988-scale events is also apparent in observed fires for the last two decades (Fig. S5). By about 2075, potential annual area burned regularly exceeds the signature 1988 event, often by a large margin. By then, forest ecosystems in the GYE, and the fuels and fire responses they support, would likely have been transformed by changing climate and disturbance and moved outside the bounds of the modeled climate–fire relationship.

Fire rotations (FRs), which exceed 120 y throughout most of the GYE before 1990, are in transition to shorter periods across all scenarios by the first decades of the 21st century (Fig. 3). Downscaled climate predictions from all three GCMs were qualitatively similar but differed somewhat with respect to mid-century timing of fire-regime shifts. For 2005–2034, FRs begin to fall below 60 y in portions of the landscape for all scenarios, although the rate of change varies; differences in precipitation among scenarios have greater influence on fire early on, whereas effects of high temperatures dominate late in the century. Spatial patterns are similar across scenarios, with FRs decreasing sooner and to a greater extent in the northwestern areas of the GYE. By midcentury, FRs are <20 y throughout the majority of the GYE, except for small portions to the southeast (Fig. 3). By end of century, climatic conditions associated with large fires are the norm (Fig. S2), and FRs <10 y are projected across the GYE for all three GCMs (Fig. 3); however, by the time such short fire rotations could be driven by climate, fuel limitations would be expected to constrain fire occurrence and area burned.

Discussion

Our findings indicate that GYE forests are rapidly approaching a threshold beyond which fire occurrence and extent are likely to change the ecosystem qualitatively. Recent history shows that a shift in spring and summer temperature (March–August) of just over 0.5 °C above the 1961–1990 average distinguished extreme fire years from most others in the Northern Rockies, and increases in average spring and summer temperatures predicted by 2099 are ~4.5–5.5 °C for the GCM scenarios explored here (Fig. 2 and Fig. S2). The projected changes in temperatures and fire are not consistent with persistence of the suite of conifer species that have dominated the Yellowstone landscape throughout the Holocene. Rather, the projected climate–fire regime is consistent with lower montane woodland or nonforest vegetation and implies a shift from a climate-limited to a fuel-limited system (24) by midcentury. Climate conditions conducive to large fires in the current system would occur in most years, but less biomass would be available to burn because recovery times between successive fires would be shorter. Thus, we might expect novel fire–climate–

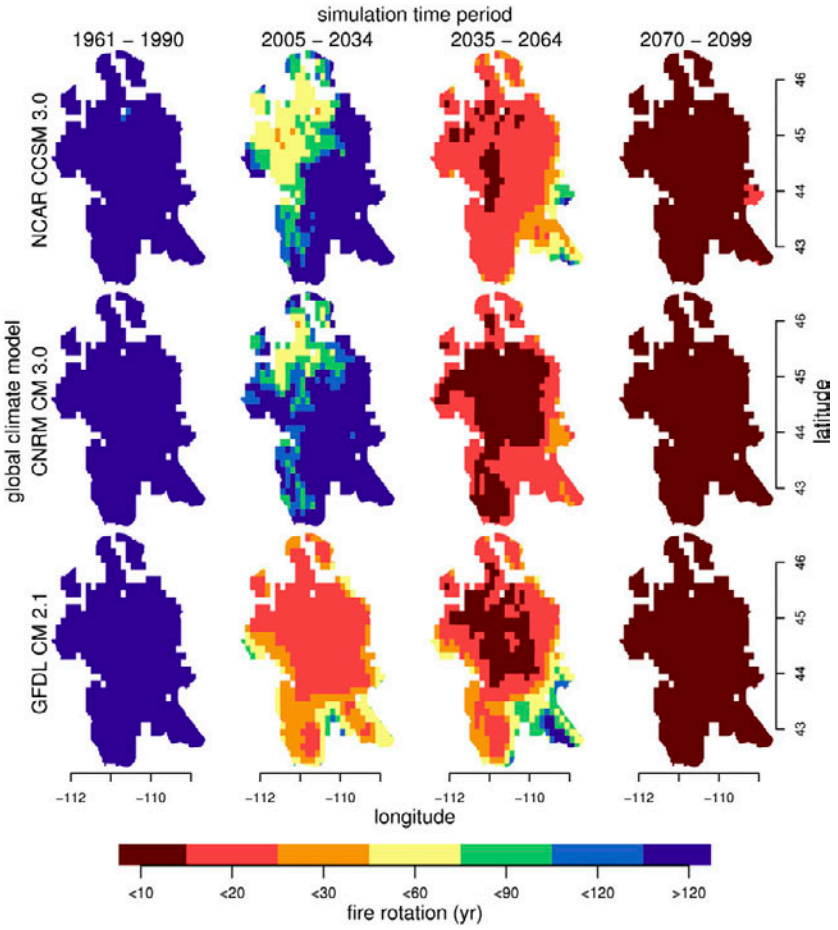

Fig. 3. Projected fire rotations calculated for 1,000 monthly gridded simulations for four 30-y periods across three downscaled GCM SRES A2 climate scenarios.

vegetation relationships, suggesting that the GYE is approaching a tipping point (i.e., critical change in temperature and moisture deficit) that could be exceeded by mid-21st century.

Our results are consistent with predictions for increased temperature-driven fire activity in other regions (20, 21, 23, 42, 43) but also suggest that future climate–fire dynamics may differ from those observed in the past. Numerous studies demonstrate that climate and fire have varied substantially in the GYE throughout the past 10,000 y. During the early Holocene, increased summer temperature was associated with increased fire frequency on the central plateau in Yellowstone National Park, and the fire return interval declined to 75–100 y for several millennia (44). During the past 1,300 y, large fires on the central plateau occurred in decades including the driest years, and widespread burning (>10,000 ha) occurred at 150- to 300-y intervals (45). During the past 2,650 y in forest–steppe vegetation of northern Yellowstone, fire intervals averaged 75 y, but fire-free intervals of several centuries were detected twice (35). Thus, climate and fire regimes have varied considerably in the past. Nonetheless, our models indicate that, by the middle of the 21st century, forests of the GYE may regularly experience climatic conditions that exceed the most extreme years in the instrumental and paleoecological record. Our models also predicted geographic differences in the timing of predicted transitions in fire regimes, notably an earlier onset of shorter fire rotations in the northwestern portions of the region. Other studies have noted spatial variation in precipitation and fire regimes in the GYE (e.g., refs. 34 and 46–49), and geographic differences in fire regimes are likely to be observed in the future.

Uncertainty in predicted climate–fire relationships increases as climate conditions move outside the historical range of variability, and predictions for the latter 21st century must be interpreted with care. Our fire models will become increasingly poor guides as current and future climates—and the fuel conditions that support current climate–fire relationships—diverge. This is true to some extent for any statistical model given the lack of recent historical analogs and the currently highly nonlinear climate–fire relationship in the study area, and predicted fire activity (especially beyond 2050) must be interpreted in the context of key assumptions. First, the statistical models of fire occurrence and area burned are based primarily on fires in conifer forests (which dominate the vegetated area) given present-day climate and vegetation; predicted future climate diverges substantially from that used for model development. Second, the nature of feedbacks from vegetation to future fire activity is a critical unknown. Area burned cannot increase indefinitely because changing fuels will eventually limit fire occurrence (50). This feedback is not included in our models but will become an increasingly important influence on fire in the latter half of the century. Following severe fire, subsequent fire activity is reduced for some time because fuels are sparse. Younger forests will burn readily in extreme fire weather, as observed during the 1988 Yellowstone fires when regenerating saplings in *Pinus contorta* stands <10 y old carried crown fire (4, 51). However, fuel quantity will diminish as the time for vegetation recovery between fires declines. Third, our study used average conditions within 12-km × 12-km grid cells and cannot predict variation in fire dynamics (e.g., effects of local topography or subgrid cell FRs) at finer spatial scales. Finally, our study did not consider variation in fire severity, and we have not considered potential interactions with other disturbances, such as outbreaks of native bark beetles (Dendroctonae) (52, 53).

Anticipating vegetation shifts in the GYE under altered climate–fire regimes is complex and beyond the scope of this study. However, fire can catalyze rapid shifts in plant communities when climate conditions change sufficiently to favor postfire establishment of different species (e.g., ref. 54), and such dynamics have already been observed elsewhere (55–57). Warming temperatures alone are expected to cause declines in suitable habitat for some conifers now common in the GYE, even if precipitation also increases (58–60). In the GYE, projected changes in temperature reach the historical differences in temperature between subalpine forest (with an historical fire rotation >100 y) and lower montane forest (with an historical fire rotation <30 y) by the end of the century. Following fire, tree species that currently occupy lower elevations in the GYE (e.g., *Pseudotsuga menziesii*, *Populus tremuloides*) could potentially expand upslope on suitable substrate, as documented for andesite substrates in the GYE during the early Holocene (61). Although the paleoecological record has revealed remarkable resilience of GYE vegetation to a wide range of climate and fire regimes (e.g., refs. 44 and 61), our study suggests that future changes in climate and fire rotations could preclude conifer regeneration and convert currently forested areas to woodland or nonforest. Future research should prioritize understanding potential postfire successional trajectories.

Conclusions

Continued warming could completely transform GYE fire regimes by the mid-21st century, with profound consequences for many species and for ecosystem services including aesthetics, hydrology, and carbon storage. The conditions associated with extreme fire seasons are expected to become much more frequent, with fire occurrence and area burned exceeding that observed in the historical record or reconstructed from paleoproxy records for the past 10,000 y. Even in years without extreme fire events, average annual area burned is projected to increase, and years with no large fires—common until recently—are projected to become increasingly rare. The timing and spatial location of such changes varied somewhat among the three GCMs used in this study, but the models converged by the latter part of the century. The magnitude of predicted increases in fire occurrence and area burned suggests that there is a real likelihood of Yellowstone's forests being converted to nonforest vegetation during the mid-21st century because reduced fire intervals would likely preclude postfire tree regeneration. A change in dominant vegetation would also cause the GYE to shift from a climate- to a fuel-limited fire regime (24). We suggest that the climate–fire system is a tipping element that may qualitatively change the flora, fauna, and ecosystem processes in this landscape and could be indicative of similar changes in other subalpine or boreal forests.

Methods

Spatial and Temporal Domain. The spatial domain for developing the climate–fire statistical models is a 1°/8° latitude/longitude grid for the Northern Rocky Mountains (n = 2,309 grid cells, ~12-km × 12-km cell size; Fig. S1). We used this larger region because it encompasses the GYE and includes multiple fire occurrences across a broad range of representative climate conditions. Statistical models were estimated for the entire domain and then applied and evaluated for the subsample comprising the GYE (n = 578). The temporal domain for model estimation included monthly data from 1972 to 1999, defined by the overlap in availability of high-quality gridded historical observed climate datasets and a comprehensive gridded fire history for the region. Thus, the statistical models were fit for 775,824 data points (2,309 grid cells × 28 y × 12 mo/y). See *SI Text* for study area description and data sources.

Statistical Models of Climate–Fire Relationships. We developed three probabilistic statistical models relating observed fires to climatic conditions for 1972–1999. Logistic regression was used to predict the probability of a fire >200 ha (henceforth "fire") occurrence in each grid cell by month. Conditional Poisson lognormal models were then estimated to predict the number (≥1) of fires given that fire occurred, with a covariate derived from the logistic regression. Finally, the area burned in each fire was predicted using a GPD fit to observed fires, using a climatic covariate. The overall statistical modeling approach is summarized as

$$\textbf{Expected Area Burned} = P(\theta(X)) \times \hat{C}(\theta \,|\, \text{fire} > 0) \times \hat{A}(X \,|\, \text{fire} = 1),$$

where θ is the linear estimator from a logistic regression on variables $\mathbf{X}$ for a given grid cell and month, $\mathbf{P}$ is the probability of fire where

$$\mathbf{P} = \exp(\theta) / (1 + \exp(\theta)),$$

$\hat{\mathbf{C}}(\boldsymbol{\theta} \,|\, \mathbf{fire} > \mathbf{0})$ is the expected number of fires given that fire occurs (≥1) estimated by a set of Poisson lognormal models conditioned on $\boldsymbol{\theta}$, and $\hat{\mathbf{A}}$ is the expected burned area per fire estimated by a GPD model as a function of variates $\mathbf{X}$. See *SI Text* for full model descriptions and cross-validation results.

Projected 21st Century Forest Fire Regimes in the GYE. Three AR4 GCMs (NCAR CCSM 3.0, CNRM CM 3.0, and GFDL CM 2.1) forced with a medium-high emissions pathway (SRES A2) (38) were used for climate predictions. For current and future climate, we used GCM runs downscaled to the North American Land Data Assimilation System (LDAS) (62) 1°/8° latitude/longitude grid (henceforth grid) to force hydrologic simulations using VIC, providing a suite of hydroclimatic variables (37).

We used our statistical models to simulate fire occurrence for the GYE (n = 578 grid cells) for 1951–2099, using downscaled hydroclimate for each GCM run. We estimated fires and area burned for 1,000 simulations per grid cell and month and then compared predictions with the historical record (Fig. 2). The actual historical record is only one possible outcome of a complex system, and the models will not reproduce the historical record exactly. However, observed fire should be within the range of outcomes represented by the simulations. The ability to generate an arbitrary number of simulations allowed us to estimate changes in extremes as well as mean fire activity and to estimate quantiles of expected fire activity.

As noted above, climate–fire interactions in GYE forests are such that small changes in model specifications can produce divergent outcomes in fire activity, especially for climate that exceeds the historic range of variability. To produce conservative future estimates of fire activity, we constrained our models by assuming that historically observed fire–climate relationships within Northern Rockies forests describe the most extreme scenarios possible at any point in space and time within the GYE. Thus, for our GCM-driven fire projections, we required that $\mathbf{P(\theta)}$ never exceed the maximum calculated using historical climate (24%), Poisson lognormal distributions never exceed the extremes calculated for historic climate (i.e., the probability of observing multiple large fires does not increase for θ above the historic maximum), the maximum number of fires burning in a single grid cell can never exceed the historic maximum (5), the GPD scale parameter never exceeds the historic maximum (i.e., scale does not increase with normalized cumulative water–year moisture deficit greater than the 1972–1999 maximum), fires never exceed the observed historic maximum area burned per fire (173 kha), and total area burned by multiple fires ignited in the same year and grid cell can never exceed the observed historic maximum (211 kha). These constraints require that, for any point in space and time, the number and size of fires simulated cannot exceed the maximum observed in the recent record and the probability of observing extremes in fire number and size cannot increase as climate exceeds historically observed extremes. Only increases in the frequency and spatial extent of extreme climate conditions are allowed to drive increases in fire.

In addition, whereas available unburned vegetated area is seldom a binding constraint on GYE burned area, we anticipate that it will become so in the future. Many simulated fires burn only a portion of a cell, but some fires burn all of the vegetated area within a cell or are larger than the cell itself. For each fire simulation, we allocate the burned area of fires starting in a grid cell to the vegetated area in that grid cell first and then to immediately adjacent cells. Where multiple fires would burn together, the total burned area is limited to the available vegetated area. Fire rotations were then estimated for simulated fire histories following Baker (10):

$$\text{FR} = t \times A \times \left(\sum_{i=1}^{n} a_i \right)^{-1},$$

where t is the simulation period in years, A is total landscape area, and a is the area of fire i of n total fires observed over period t. For each climate scenario, FR was estimated for each grid cell over 1,000 simulations for each of four 30-y periods (1961–1990, 2005–2034, 2035–2064, and 2070–

2099), so that t = 30,000 for each 30-y period. Some fire was always present for each period t. Total landscape area was estimated to be the average per-grid cell vegetated area using LANDFIRE vegetation data (0.89 × cell area) (63).

ACKNOWLEDGMENTS. We thank A. Keyser, K. Lubetkin, T. Das, F. Munoz-Arriola, and D. Lettenmaier for assistance with data processing, visualization, hydrologic simulations, and historical gridded climate data. We acknowledge the Program for Climate Model Diagnosis and Intercomparison and the World Climate Research Program's Working Group on Coupled Modeling for their roles in making available the World Climate Research Program Coupled Model Intercomparison Project phase 3 multimodel dataset, supported by the US Department of Energy. We thank C. D. Allen, F. S. Chapin, D. C. Donato, C. Whitlock, and M. D. Dettinger for comments that improved this manuscript. This research was funded by Joint Fire Science Program Project 09-3-01-47, US Forest Service Southern Research Station Joint Venture Agreement 07-CA-11330143-129, and National Oceanic and Atmospheric Administration Grant NA10OAR4310217.

1. Bowman DMJS, et al. (2009) Fire in the Earth system. *Science* 324:481–484.
2. Krawchuk MA, Moritz MA, Parisien M-A, Van Dorn J, Hayhoe K (2009) Global pyrogeography: The current and future distribution of wildfire. *PLoS ONE* 4:e5102.
3. Johnson EA (1992) *Fire and Vegetation Dynamics* (Cambridge Univ Press, New York).
4. Turner MG, Romme WH (1994) Landscape dynamics in crown fire ecosystems. *Landscape Ecol* 9:59–77.
5. Schoennagel T, Veblen TT, Romme WH (2004) The interaction of fire, fuels, and climate across Rocky Mountain forests. *Bioscience* 54:661–676.
6. Whitlock C, et al. (2008) Long-term relations among fire, fuel, and climate in the northwestern US based on lake-sediment studies. *Int J Wildland Fire* 17:72–83.
7. Bessie WC, Johnson EA (1995) The relative importance of fuels and weather on fire behavior in subalpine forests. *Ecology* 76:747–762.
8. Fauria MM, Johnson EA (2008) Climate and wildfires in the North American boreal forest. *Philos Trans R Soc B* 363:2317–2329.
9. Littell JS, et al. (2010) Forest ecosystems, disturbance, and climatic change in Washington State, USA. *Clim Change* 102:129–158.
10. Baker WL (2009) *Fire Ecology in Rocky Mountain Landscapes* (Island Press, Washington, DC).
11. Kurz WA, Stinson G, Rampley GJ, Dymond CC, Neilson ET (2008) Risk of natural disturbances makes future contribution of Canada's forests to the global carbon cycle highly uncertain. *Proc Natl Acad Sci USA* 105:1551–1555.
12. Purves D, Pacala S (2008) Predictive models of forest dynamics. *Science* 320: 1452–1453.
13. Balshi MS, et al. (2009) Vulnerability of carbon storage in North American boreal forests to wildfires during the 21st century. *Glob Change Biol* 15:1491–1510.
14. Metsaranta JM, et al. (2010) Implications of future disturbance regimes on the carbon balance of Canada's managed forest (2010–2100). *Tellus Ser B Chem Phys Meteorol* 62(SI):719–728.
15. Intergovernmental Panel on Climate Change (IPCC) (2007) *Climate Change 2007: The Physical Science Basis* (IPCC Secretariat, WMO, Geneva).
16. Skinner WR, Shabbar A, Flannigan MD, Logan K (2006) Large forest fires in Canada and the relationship to global sea surface temperatures. *J Geophys Res* 111:D14106.
17. Tymstra C, et al. (2007) Impact of climate change on area burned in Alberta's boreal forest. *Int J Wildland Fire* 16:153–160.
18. Flannigan MD, Krawchuck MA, de Groot WJ, Wotton BM, Gowman LM (2009) Implications of changing climate for global wildland fire. *Int J Wildland Fire* 18:483–507.
19. Liu YQ, Stanturf J, Goodrick S (2009) Trends in global wildfire potential in a changing climate. *Forest Ecol Manage* 259(SI):685–697.
20. Pechony O, Shindell DT (2010) Driving forces of global wildfires over the past millennium and the forthcoming century. *Proc Natl Acad Sci USA* 107:19167–19170.
21. Wotton BM, Nock CA, Flannigan MD (2010) Forest fire occurrence and climate change in Canada. *Int J Wildland Fire* 19:253–271.
22. Westerling AL, Brown TJ, Gershunov A, Cayan DR, Dettinger MD (2003) Climate and wildfire in the western United States. *Bull Am Meteorol Soc* 84:595–604.
23. Girardin MP, et al. (2009) Heterogeneous response of circumboreal wildfire risk to climate change since the early 1900s. *Glob Change Biol* 15:2751–2769.
24. Littell JS, McKenzie D, Peterson DL, Westerling AL (2009) Climate and wildfire area burned in western U.S. ecoprovinces, 1916–2003. *Ecol Appl* 19:1003–1021.
25. Paine RT, Tegner MJ, Johnson EA (1998) Compounded perturbations yield ecological surprises. *Ecosystems (N Y)* 1:535–545.
26. Turner MG (2010) Disturbance and landscape dynamics in a changing world. *Ecology* 91:2833–2849.
27. Lenton TM, et al. (2008) Tipping elements in the Earth's climate system. *Proc Natl Acad Sci USA* 105:1786–1793.
28. Johnstone JF, Hollingsworth TN, Chapin FS, III, Mack MC (2010) Changes in fire regime break the legacy lock on successional trajectories in Alaskan boreal forest. *Glob Change Biol* 16:1281–1295.
29. Greene DF, Johnson EA (1999) Modeling recruitment of *Populus tremuloides*, *Pinus banksiana*, and *Picea mariana* following fire in the mixedwood boreal forest. *Can J For Res* 29:462–473.
30. Johnstone JF, Chapin FS, III (2006) Fire interval effects on successional trajectory in boreal forests of Northwest Canada. *Ecosystems (N Y)* 9:268–277.
31. Westerling AL, Hidalgo HG, Cayan DR, Swetnam TW (2006) Warming and earlier spring increase western U.S. forest wildfire activity. *Science* 313:940–943.
32. Heyerdahl EK, Morgan P, Riser JP, 2nd (2008) Multi-season climate synchronized historical fires in dry forests (1650–1900), northern Rockies, U.S.A. *Ecology* 89: 705–716.
33. Morgan P, Heyerdahl EK, Gibson CE (2008) Multi-season climate synchronized forest fires throughout the 20th century, northern Rockies, U.S.A. *Ecology* 89:717–728.
34. Millspaugh SH, Whitlock C, Bartlein PJ (2004) *After the Fires: The Ecology of Change in Yellowstone National Park*, ed Wallace LL (Yale Univ Press, New Haven), pp 10–28.
35. Whitlock C, et al. (2008) A 2650-year-long record of environmental change from northern Yellowstone National Park based on a comparison of multiple proxy data. *Quat Int* 188:126–138.
36. Huerta MA, Whitlock C, Yale J (2009) Holocene vegetation-fire-climate linkages in northern Yellowstone National Park, USA. *Paleogoeg Paleoclimatol Paleoecol* 271: 170–181.
37. Liang X, Lettenmaier DP, Wood EF, Burges SJ (1994) A simple hydrologically based model of land surface water and energy fluxes for general circulation models. *J Geophys Res* 99:14,415–14,428.
38. Intergovernmental Panel on Climate Change (IPCC) (2000) *Special Report on Emissions Scenarios: A Special Report of Working Group III of the Intergovernmental Panel on Climate Change* (Cambridge Univ Press, New York).
39. Cayan D, et al. (2009) *Climate Change Scenarios and Sea Level Rise Estimates for the California 2008 Climate Change Scenarios Assessment.* PIER Research Report, CEC-500-2009-014 (Sacramento, CA).
40. Ropelewski CF, Halpert MS (1986) North American precipitation and temperature patterns associated with the El Nino/Southern Oscillation (ENSO). *Mon Weather Rev* 114:2352–2362.
41. Le Quéré C, et al. (2009) Trends in sources and sinks of carbon dioxide. *Nat Geosci* 2: 831–836.
42. Flannigan MD, Stocks BJ, Wotton BM (2000) Climate change and forest fires. *Sci Total Environ* 262:221–229.
43. Westerling AL, Bryant BP (2008) Climate change and wildfire in California. *Clim Change* 87:s231–s249.
44. Millspaugh SH, Whitlcok C, Barlein PJ (2000) Variations in fire frequency and climate over the past 17 000 yr in central Yellowstone National Park. *Geology* 28:211–214.
45. Higuera PE, Whitlock C, Gage JA (2010) Linking tree-ring and sediment-charcoal records to reconstruct fire occurrence and area burned in subalpine forests of Yellowstone National Park, USA. *Holocene* 21:327–341.
46. Whitlock C, Bartlein PJ (1993) Spatial variations of Holocene climatic change in the Yellowstone Region. *Quat Res* 39:231–238.
47. Schoennagel T, et al. (2005) ENSO and PDO variability affect drought-induced fire occurrence in Rocky Mountain subalpine forests. *Ecol Appl* 15:2000–2014.
48. Gray ST, Fastie C, Jackson ST, Betancourt JL (2004) Tree-ring based reconstructions of precipitation in the Bighorn Basin, Wyoming, since AD 1260. *J Climatol* 17:3855–3865.
49. Gray ST, Graumlich LJ, Betancourt JL (2007) Annual precipitation in the Yellowstone National Park region since AD 1173. *Quat Res* 68:18–27.
50. Krawchuk MA, Cumming SG (2011) Effects of biotic feedback and harvest management on boreal forest fire activity under climate change. *Ecol Appl* 21:122–136.
51. Turner MG, Hargrove WH, Gardner RH, Romme WH (1994) Effects of fire on landscape heterogeneity in Yellowstone National Park, Wyoming. *J Veg Sci* 5:731–742.
52. Lynch HJ, Renkin RA, Crabtree RL, Moorcroft PR (2006) The influence of previous mountain pine beetle (*Dendroctonus ponderosae*) activity on the 1988 Yellowstone fires. *Ecosystems (N Y)* 9:1318–1327.
53. Simard M, Romme WH, Griffin JM, Turner MG (2011) Do mountain pine beetle outbreaks change the probability of active crown fire in lodgepole pine forests? *Ecol Monogr* 81:3–24.
54. Cwynar LC (1987) Fire and the forest history of the North Cascade Range. *Ecology* 68: 791–802.
55. Johnstone JF, Chapin FS, III (2003) Non-equilibrium succession dynamics indicate continued northern migration of lodgepole pine. *Glob Change Biol* 9:1401–1409.
56. Wirth C, Lichstein JW, Dushoff J, Chen A, Chapin FS, III (2008) White spruce meets black spruce: dispersal, postfire establishment, and growth in a warming climate. *Ecol Monogr* 78:489–505.
57. Frelich LE, Reich PB (2010) Will environmental changes reinforce the impact of global warming on the prairie-forest border of central North America? *Front Ecol Environ* 8:371–378.
58. Monserud RA, Yang Y, Huang S, Tchebakova N (2008) Potential change in lodgepole pine site index and distribution under climatic change in Alberta. *Can J For Res* 38: 343–352.
59. Schrag AM, Bunn AG, Graumlich LJ (2008) Influence of bioclimatic variables on treeline conifer distribution in the Greater Yellowstone Ecosystem: Implications for species of conservation concern. *J Biogeogr* 35:698–710.
60. Coops NC, Waring RH (2011) A process-based approach to estimate lodgepole pine (*Pinus contorta* Dougl.) distribution in the Pacific Northwest under climate change. *Clim Change* 105:313–328.
61. Whitlock C (1993) Postglacial vegetation and climate of Grand Teton and southern Yellowstone National Parks. *Ecol Monogr* 63:173–198.
62. Mitchell KE, et al. (2004) The multi-institution North American Land Data Assimilation System (NLDAS): Utilizing multiple GCIP products and partners in a continental distributed hydrological modeling system. *J Geophys Res* 109:D07S90.
63. Rollins M (2009) LANDFIRE: A nationally consistent vegetation, wildland fire, and fuel assessment. *Int J Wildland Fire* 18:235–249.

Supporting Information

Westerling et al. 10.1073/pnas.1110199108

SI Text

Study Area Description. Centered on Yellowstone National Park, the Greater Yellowstone ecosystem (GYE) encompasses nearly 80,000 km^2 in northwestern Wyoming, Montana, and Idaho (Fig. S1) and also includes Grand Teton National Park, the National Elk Refuge, seven national forests, and part of the Wind River Indian Reservation. Pre-Columbian flora and fauna are largely intact, and fire and vegetation dynamics are well understood. About 60% of our GYE study area is forested, with *Pinus contorta* var. *latifolia* dominating the high-elevation plateaus; *Picea engelmanii*, *Abies lasiocarpa*, and *Pinus albicaulis* abundant at higher elevations; and *Pseudotsuga menziesii* common at lower elevations. Localized stands of *Populus tremuloides* also occur in the landscape, and the forests transition to sagebrush–grasslands (dominated by *Artemisia tridentata*) as elevation declines. Paleoecological studies document changes in vegetation and fire during the past 17,000 y, but conifer forests have persisted and dominated for the past 10,000 y (1). Fire-return intervals have been nonstationary—varying from ∼100–300 y throughout the Holocene—and highly sensitive to climate (1–3); vegetation feedbacks (i.e., fuel controls) have played a lesser role (4, 5). Fire-return intervals in lower elevation forest–steppe vegetation are also thought to be long (75–100 y) (1, 6). The 1988 Yellowstone Fires burned ∼709,000 ha in our GYE study area during the driest summer on record (7) (Fig. S6) and marked a new era of increased regional fire activity. Large, severe fires were generally infrequent during the past 300 y in the GYE, although extensive fires occurred in the early 1700s and mid-1800s (8, 9).

Data Sources and Description. ***Fire history.*** Fire histories for National Park Service (NPS) and Bureau of Indian Affairs (BIA) lands were obtained from the US Department of Interior (2008 Fire CDROM) and for US Forest Service (USFS) lands from the US Department of Agriculture (http://fam.nwcg.gov/fam-web/kcfast/mnmenu.htm) and used to update and extend Westerling et al.'s fire history (10). Westerling et al. assembled a fire history for western US forest areas managed by NPS and USFS, including fires >400 ha reported to burn in forest areas through 2003 and classified as "suppression" or "action" fires (10). We used the same methodology here to create a comprehensive history of fires >200 ha reported burning in all vegetation types by NPS, USFS, and BIA through 2008. Fires classified as suppression or action fires were retained to create a database for estimating Poisson lognormal and generalized Pareto distributions (GPD) and aggregated to monthly gridded presence/absence data for estimating logistic regression models. Most of the suppression fires were actually quite large because suppression was ineffective during periods of extreme fire weather.

In general, fires <200 ha in size are the most numerous, but these fires account for a small fraction of area burned and data quality is often poor, with missing data fields and erroneous or incomplete location information common. By restricting our sample to fires above this size threshold, we retained the fires accounting for most of the burned area while making quality assurance feasible. Furthermore, mid- to large-sized fires tend to have better data quality, probably because their economic and ecological consequences bring greater scrutiny. Records for the very largest fires require special care; because of their scale they dominate the burned area record, and multiple agencies and land management units can be involved in suppression actions on the same fire, resulting in multiple and conflicting bookkeeping entries for accounting purposes. Fire records from NPS, USFS, and BIA were examined, and obvious duplications and errors were corrected (10). In addition, individual records corresponding to very large fires and fire complexes burning in the GYE in 1988 were compared with Rothermel et al.'s fire spread maps and summary statistics (11). Large duplicate fire entries for the North Fork complex were removed, and burned area and ignitions for the Clovermist complex were adjusted to correspond to mapped ignitions and final burned areas for those fires. Our sum for total burned area in 1988 was within 1000 ha (0.15%) of the burned area mapped by Rothermel et al. (∼683,000 ha). In addition, our larger GYE study region also included fires on the periphery, which accounted for another 26,000 ha. Thus, we used a total 1988 GYE burned area of 709,000 ha in our analyses.

Although we included fires burning in all vegetation types, forest fires dominated, accounting for 89% of burned area. Whereas our primary interest was in forest fires, fires that ignite in different vegetation types (e.g., sagebrush–grasslands) can burn into forested areas, so it was important for this analysis that we include fires in adjacent nonforested areas. We excluded from our analysis human or naturally ignited fires used to achieve fuel management objectives and fires for which no classification data were available; these excluded fires accounted for ∼3% of the total burned area for all fire types in the Northern Rockies through 1999. Excluded fires were typically management fires ignited (by lightning or by humans) in forests during years with otherwise relatively low fire risk (e.g., 1981, 1998, and 1999) and/or at times of the year (e.g., late June, early July) not typical for large action fires in the Northern Rockies. Because the timing and ultimate size of these management fires were strongly influenced by factors other than climate, and because of their relatively small share of burned area, their exclusion is not likely to significantly or qualitatively affect the results of this analysis.

Land surface characteristics. Gridded topographic information derived from the GTOPO30 Global 30 Arc Second (∼1 km) Elevation Data Set (elevation, slope, aspect) and coarse vegetation types using the University of Maryland vegetation classification scheme were accessed online from the North American Land Data Assimilation System (LDAS) (http://ldas.gsfc.nasa.gov) (12).

Detailed existing vegetation type data were accessed online from the LANDFIRE project (http://www.landfire.gov) (13). These data were scaled up from 30- and 120-m polygons to provide summary statistics for each 12-km grid cell of the fraction vegetated in major GYE forest types (*P. contorta*, *P. menziesii*, *Pinus flexilis*, *P. engelmanii*, *A. lasiocarpa*, *P. albicaulis*, and *P. tremuloides*), as well as sagebrush–grasslands and meadows (Fig. S1).

Climatic and hydrologic data. Gridded daily climate data (temperature, precipitation, and wind speed) derived from historical (1950–1999) station observations were obtained from Santa Clara University (http://www.engr.scu.edu/∼emaurer/data.shtml) (14). Gridded daily climate data derived from observations at a subset of stations using the index station method (15) for 1961–2005 were obtained from the University of Washington National Hydrologic Prediction System (NHPS) (http://www.hydro.washington.edu/forecast/westwide/). The NHPS data do not incorporate all of the potentially available station data but are updated more frequently than the Maurer et al. (14) dataset, providing longer time series for use in model validation, and use stations with high-quality records.

Simulated future daily temperature and precipitation values were obtained directly from modeling groups contributing to the

World Climate Research Program (WCRP)'s Coupled Model Intercomparison Project phase 3 (CMIP3) multimodel dataset for three GCM runs—National Center for Atmospheric Research (NCAR) CCSM 3.0 run 5, Centre National de Recherches Météorologiques (CNRM) CM 3.0 run 1, and Geophysical Fluid Dynamics Laboratory (GFDL) CM 2.1 run 1—forced with the SRES A2 emissions pathway (16) (see http://www-pcmdi.llnl.gov/ for GCM scenario metadata). Similarly, 20th century simulations ("20C3M")—NCAR CCSM 3.0 run 5, CNRM CM 3.0 run 1, and GFDL CM 2.1 run 2—were obtained directly and downscaled to the grid to provide simulations for the historic period. NCAR CCSM3.0 daily data were accessed via the Earth System Grid (http://www.earthsystemgrid.org) with assistance from Gary Bates (NCAR). Daily CNRM CM3.0 data were obtained via special permission granted to Scripps Institution of Oceanography (SIO) from CNRM. GFDL CM2.1 data were obtained from the GFDL ftp server nomads with permission granted to SIO by Tom Delworth at GFDL. GCM simulations were downscaled to the LDAS grid using the Bias Corrected Constructed Analogs method (17). (See Fig. S2 for a summary of the climate scenarios.)

Wind speed data for 1950–1999 were accessed online from the National Centers for Environmental Prediction Reanalysis project (http://www.esrl.noaa.gov/psd/data/reanalysis/) and used to calculate a monthly wind speed climatology interpolated to the LDAS grid.

We used daily climate data, LDAS (historical) vegetation and topography, and climatological winds to force the Variable Infiltration Capacity (VIC) hydrologic model at a daily time step in water balance mode, resulting in a suite of gridded hydroclimatic variables, including actual evapotranspiration (AET), relative humidity, soil moisture, and snow water equivalent (18). Because VIC does not output readily usable potential evapotranspiration (PET), PET was estimated using the Penman–Montieth equation with the same forcing and output data and used to calculate moisture deficit (D = PET − AET) (10, 19, 20). All variables were aggregated to monthly average or cumulative values, as appropriate.

Using these predicted hydroclimatic variables, we created a monthly historical record for each grid cell (n = 2,309 cells; Fig. S1) of number of fires >200 ha, fire presence (i.e., 1 if number of fires >0, 0 otherwise), and area burned; along with historic temperature, precipitation, and simulated hydrologic variables; topographic variables such as mean and SD of elevation, slope, and aspect; and LANDFIRE vegetation types.

Statistical Models of Climate–Fire Relationships. ***Predicting fire occurrence.*** Fire occurrence on the LDAS grid was predicted using a logistic regression model with Maurer et al.'s (14) climate data, hydrologic data we simulated with VIC, and GTOPO topographic data from LDAS, as predictors. All values were by grid cell unless otherwise specified. The precise model specification is

$$\begin{aligned}\mathbf{Logit(P)} &= \mathbf{\log(P/(1-P))}\\ &= \boldsymbol{\beta}\times[\mathbf{1 + month + elevsd + G(elev) +}\\ &\quad \mathbf{aspestN + aspectE + G(lat, lon) +}\\ &\quad \mathbf{Tavg + Tnr + G(Pree) +}\\ &\quad \mathbf{G(D00) + G(D0) + D1 + D2 + (D0\times elev)}],\end{aligned}$$

where functions **G(X)** are semiparametric smooth functions (21) such as piecewise polynomial and thin plate spline transformations of variables **X**, as described in Preisler and Westerling (22), **month** is a smoothed curve fit to average monthly regional historical fire occurrence, **elevsd**, **G(elev)** are the SD and second-order polynomial transformation of elevation, **aspectN** and **aspectE** are transformations of GTOPO30 aspect into north–south and east–west components, **G(lat, lon)** is a matrix describing a thin plate spline that estimates a spatial surface as a function of longitude and latitude (22, 23) [modules for fitting thin-plate splines within R were downloaded from the Internet (Geophysical Statistical Project; information available online at http://www.cgd.ucar.edu/stats/Software/Fields)], **Tavg** is the monthly mean bias-corrected temperature, **Tnr** is the regionally (Northern Rockies) averaged March through August temperature, **G(Prec)** is a second-order polynomial transformation of normalized monthly precipitation, **G(D00)** is a third-order polynomial of normalized cumulative water–year moisture deficit, **G(D0)** is a second-order polynomial of normalized monthly moisture deficit, **D1** and **D2** are the 1- and 2-mo leading normalized monthly moisture deficits, and **β** is a vector of parameters to be estimated.

The linear estimator for the logit(**P**) is θ. To estimate θ for the regression described above, we used the glm() function in the **stats** package in the **R** statistical computing and graphics environment (http://www.r-project.org) to estimate a generalized linear model with binomial error terms, where the predictand was 1 when a fire was observed and 0 otherwise. Candidate model specifications were compared using Akaike information criterion (AIC) statistics calculated by glm(). The AIC measures statistical models' goodness of fit while accounting for differences in model complexity and is not affected by spatial autocorrelation in the variables (24).

The best models included both local monthly temperature (**tavg**) and a regional spring and summer temperature index (**tNR**). In particular, models without the latter did not capture extremes in observed fire occurrence, both high and low. Because most area is burned during historically rare extreme events, it was crucial to derive a model that could predict the most extreme fire seasons. Correlation between **tavg** and **tNR**, although highly significant ($P < 2.2e$-16), was very low ($\rho < 0.05$). Even accounting for seasonal variations, correlation between **tNR** and **tavg** ranged from 0.01 (July) to 0.36 (April). We posit that **tNR** may be a good indicator of both the timing of spring and the length and intensity of the overall Northern Rockies fire season.

The logistic regression model specification was tested using leave-one-out cross-validation (Fig. S3). That is, for each of 28 y in 1972–1999, we estimated a separate set of model parameters, using the other 27 y to train a model that was then used to predict the 28th year. In this way we seek to avoid overfitting our model, because the model used to predict events in any given year was derived without using data contemporaneous to events it is intended to predict. Thus, the cross-validated model skill is indicative of expected out-of-sample performance. The cross-validated models did not deviate substantially from a model estimated using all of the data. Note that simulations of fire under each GCM climate scenario used a model with the same specification as described above, but with parameters calculated using all 28 y of historical data.

Predicting number of fires. To determine the number of fires given fire occurrence, we fit Poisson lognormal distributions to fire numbers observed per grid cell and month. Distributions were fit to four samples of fire data defined by breakpoints in the logit θ corresponding to observed occurrence of increased numbers of fires (<1, ≥1, ≥2, ≥3). Results were not highly sensitive to the selection of breakpoints (i.e., the probability of observing larger numbers of fires increased gradually with increasing θ). Model skill was assessed with leave-one-out cross-validation, using the cross-validated θ and associated breakpoints (Fig. S7).

Predicting fire size. To determine fire size, we used a GPD fit to the logarithm of fire size. The GPD is a "points over thresholds" model that allows us to simulate fire size distributions, in our case for fires >200 ha. The choice of a 200-ha threshold when creating our fire history was arbitrary but fit the criteria for a GPD (i.e., for samples defined above a threshold, the sample means are a linear function of the threshold values) (25). We fit a GPD to observed Northern Rockies fire sizes using the **ismev**

library in **R**. As when estimating our logistic regression, we used the AIC to compare model specifications for GPD scale and shape parameters (using our suite of climatic, hydrologic, and topographic variables). A parsimonious model with cumulative water year moisture deficit (**D00**) as a predictor for the scale parameter and a stationary shape parameter was best. For each historical fire in the Northern Rockies, we estimated random draws from the GPD as a function of **D00** and compared the distribution of simulated annual area burned for the Northern Rockies to the observed values. The close linear fit between simulated and observed quantiles of Northern Rockies log-transformed burned area (Fig. S8) indicates that the generalized Pareto is a good approximation to the distribution of observed fire sizes. Comparing the time series of observed burned area aggregated over the Northern Rockies to 1,000 simulations for each observed historic fire also indicates a good fit between the model and observations (Fig. S9). Area burned in 1988 and 1994, the two most significant fire years in the 1972–1999 model estimation period, was within 1.5 times the interquartile range of our simulations (i.e., within the middle 75% of simulations), and the model correctly predicted smaller fire sizes and lower total burned area in 1994 than in 1988, despite the greater number of fires in 1994 (102 large fires observed in 1994 versus 87 in 1988).

Leave-one-out cross-validation was not practical for assessing GPD model skill, because just 1 y in our estimation period accounted for extremes in moisture deficit and in fire sizes that accounted for a majority (55%) of area burned in the Northern Rockies (96% in the GYE). To validate our model specification, we used **D00** derived from the NHPS climate data with values through 2005. Parameters for a GPD were estimated on these data over 1972–1988 and used to simulate area burned for all observed fires from 1972 to 2005 (Fig. S9). Simulated fire sizes in the validation period (1989–2005), which included three significant fire years, fit the observed data as well as or better than during the model training period [Spearman rank correlation between the annual mean of simulations and annual observed area burned was 0.87 ($P < 2.2e\text{-}16$) for the model estimation period (1972–1988) and 0.92 ($P < 2.2e\text{-}16$) for the validation period (1989–2005)].

1. Whitlock C, et al. (2008) Long-term relations among fire, fuel, and climate in the northwestern US based on lake-sediment studies. *Int J Wildland Fire* 17:72–83.
2. Whitlock C, Shafer SL, Marlon J (2003) The role of climate and vegetation change in shaping past and future fire regimes in the northwestern US and the implications for ecosystem management. *For Ecol Manage* 178:5–21.
3. Millspaugh SH, Whitlock C, Bartlein PJ (2004) *After the Fires: The Ecology of Change in Yellowstone National Park*, ed Wallace LL (Yale Univ Press, New Haven), pp 10–28.
4. Millspaugh SH, Whitlock C, Bartlein PJ (2000) Variations in fire frequency and climate over the past 17 000 yr in central Yellowstone National Park. *Geology* 28:211–214.
5. Higuera PE, Whitlock C, Gage JA (2010) Linking tree-ring and sediment-charcoal records to reconstruct fire occurrence and area burned in subalpine forests of Yellowstone National Park, USA. *Holocene* 21:327–341.
6. Huerta MA, Whitlock C, Yale J (2009) Holocene vegetation-fire-climate linkages in northern Yellowstone National Park, USA. *Paleogoeg Paleoclimatol Paleoecol* 271: 170–181.
7. Renkin RA, Despain DG (1992) Fuel moisture, forest type, and lightning-caused fire in Yellowstone National Park. *Can J For Res* 22:37–45.
8. Romme WH, Despain DG (1989) Historical perspective on the Yellowstone fires of 1988. *Bioscience* 39:695–699.
9. Schoennagel T, Turner MG, Romme WH (2003) The influence of fire interval and serotiny on postfire lodgepole pine density in Yellowstone National Park. *Ecology* 84:1967–1978.
10. Westerling AL, Hidalgo HG, Cayan DR, Swetnam TW (2006) Warming and earlier spring increase western U.S. forest wildfire activity. *Science* 313:940–943.
11. Rothermel RC, Hartford RA, Chase CH (1994) *Fire Growth Maps for the 1988 Greater Yellowstone Area Fires.* USDA Forest Service General Technical Report INT-304 (US Department of Agriculture Forest Service Intermountain Research Station, Ogden, UT).
12. Mitchell KE, et al. (2004) The multi-institution North American Land Data Assimilation System (NLDAS): Utilizing multiple GCIP products and partners in a continental distributed hydrological modeling system. *J Geophys Res* 109:D07S90.
13. Rollins M (2009) LANDFIRE: A nationally consistent vegetation, wildland fire, and fuel assessment. *Int J Wildland Fire* 18:235–249.
14. Maurer EP, Wood AW, Adam JC, Lettenmaier DP, Nijssen B (2002) A long-term hydrologically based data set of land surface fluxes and states for the conterminous United States. *J Clim* 15:3237–3251.
15. Wood AW, Lettenmaier DP (2006) A testbed for new seasonal hydrologic forecasting approaches in the western U.S. *Bull Am Meteorol Soc* 87:1699–1712.
16. Intergovernmental Panel on Climate Change (IPCC) (2000) *Special Report on Emissions Scenarios: A Special Report of Working Group III of the Intergovernmental Panel on Climate Change* (Cambridge Univ Press, New York).
17. Maurer EP, et al. (2010) The utility of daily large-scale climate data in the assessment of climate change impacts on daily streamflow in California. *Hydrol Earth Syst Sci* 14: 1125–1138.
18. Liang X, Lettenmaier DP, Wood EF, Burges SJ (1994) A simple hydrologically based model of land surface water and energy fluxes for general circulation models. *J Geophys Res* 99:14,415–14,428.
19. Penman HL (1948) Natural evaporation from open water, hare soil and grass. *Proc R Soc Lond A Math Phys Sci* 193:120–145.
20. Monteith JL (1965) Evaporation and environment. *Symp Soc Exp Biol* 19:205–234.
21. Hastie TJ, Tibshirani R, Friedman J (2001) *The Elements of Statistical Learning: Data Mining, Inference, and Prediction* (Springer, New York).
22. Preisler HK, Westerling AL (2007) Statistical model for forecasting monthly large wildfire events in the Western United States. *J Appl Meteorol Climatol* 46:1020–1030.
23. Preisler HK, Westerling AL, Gebert KM, Munoz-Arriola F, Holmes TP (2011) Spatially explicit forecasts of large wildland fire probability and suppression costs for California. *Int J Wildland Fire* 20:508–517.
24. Burnham KP, Anderson DR (2002) *Model Selection and Multimodel Inference: A Practical Information-Theoretic Approach* (Springer, New York), 2nd Ed.
25. Coles S (2001) *An Introduction to Statistical Modeling of Extreme Values* (Springer, London).

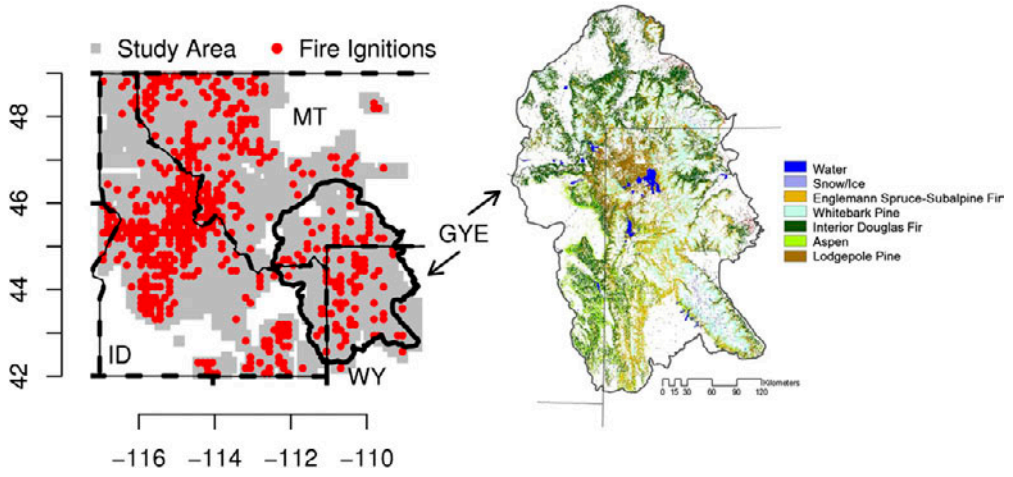

Fig. S1. Study area depicting the northern Rocky Mountain region for which statistical models relating climate to fire size were estimated (n = 2,309 grid cells) (*Left*) and the extent and dominant vegetation of the Greater Yellowstone ecosystem (*Right*). Fire ignitions (*Left*) are for large fires 1972–2005.

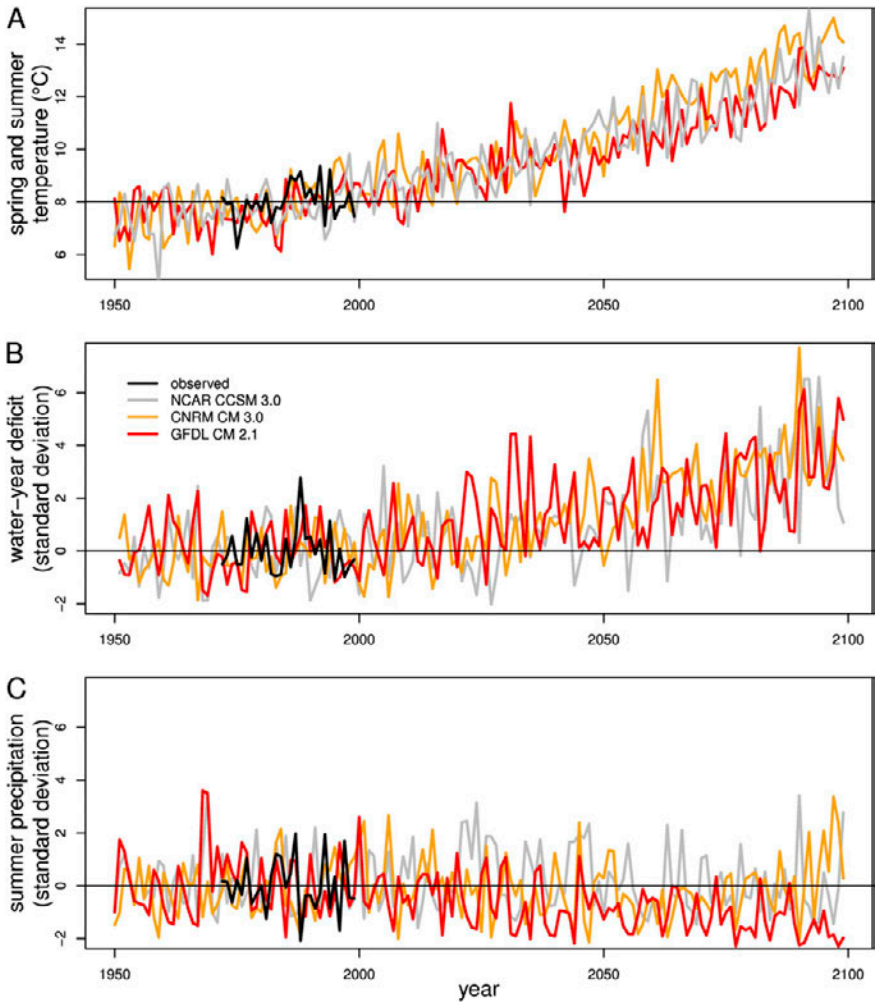

Fig. S2. (*A*) Northern Rockies regionally averaged spring and summer (March–August) temperature. (*B*) Standardized cumulative water–year (October–September) moisture deficit. (*C*) Standardized summer (July–August) precipitation. Values are derived from the instrumental record (*black*) and downscaled SRES A2 climate scenarios for three GCMs: NCAR CCSM 3.0 (*gray*), CNRM CM3.0 (*orange*), and GFDL CM2.1 (*red*).

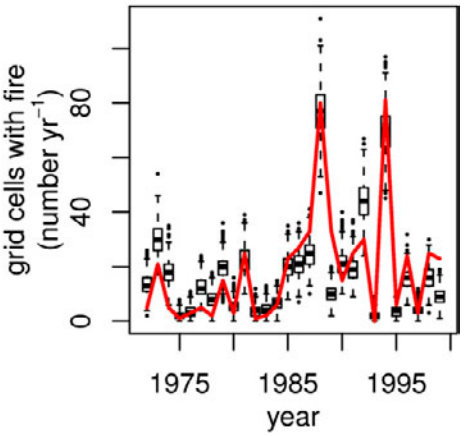

Fig. S3. Observed (*red*) and simulated (*black*) fire presence for each year from 1972 to 1999 for 2,309 Northern Rockies grid points. One thousand fire presence simulations were drawn for each month and grid cell from binomial distributions using probabilities from cross-validated logistic regressions and aggregated by year for the region.

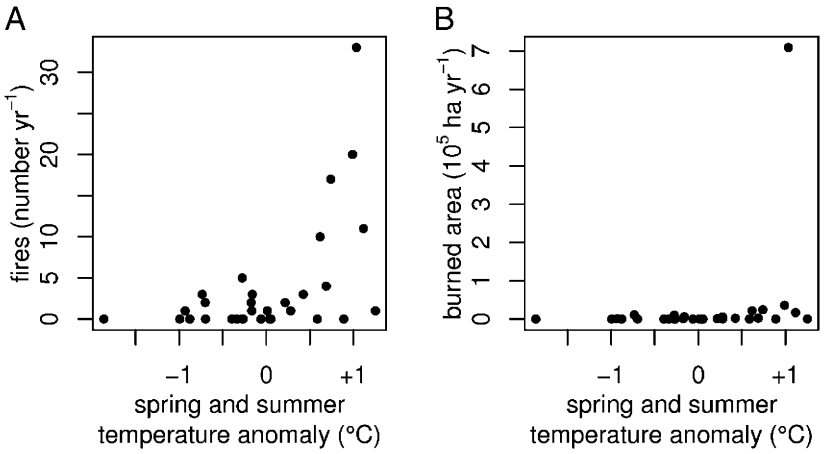

Fig. S4. (*A* and *B*) Greater Yellowstone annual number of large fires (*A*) and area burned in large fires (*B*) vs. spring and summer (March–August) temperature anomalies for 1972–2005. Fires were reported by US Forest Service, National Park Service, and Bureau of Indian Affairs as igniting in forested areas and classified as "suppression" or "action" fires.

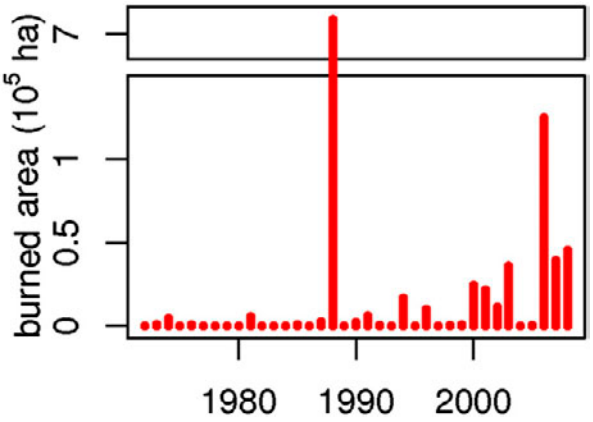

Fig. S5. Annual GYE burned area, with vertical scale truncated to highlight the apparent trend in post-1990 annual burned area.

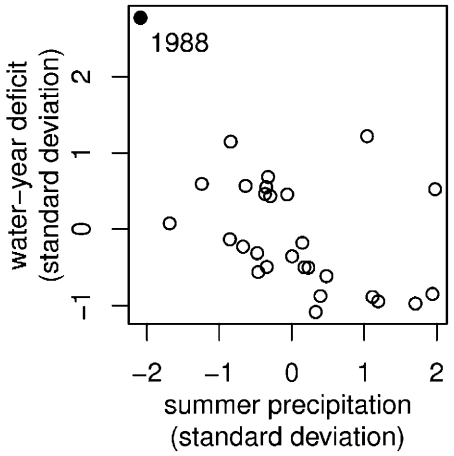

Fig. S6. GYE cumulative water–year moisture deficit versus July and August precipitation (1972–1999). The 1988 fires occurred in the driest year.

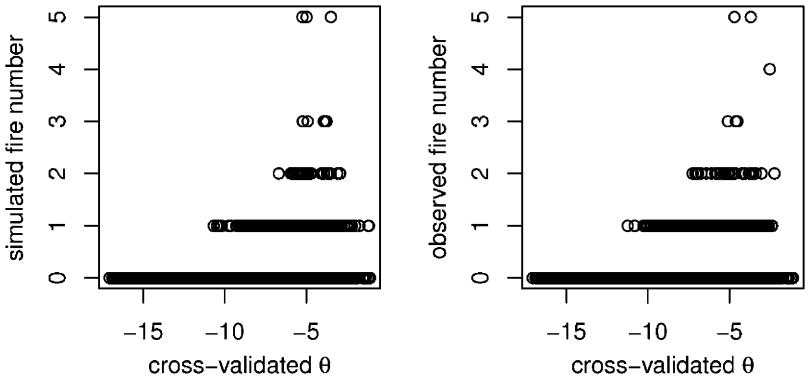

Fig. S7. Observed (*Left*) and simulated (*Right*) number of fires for each month from 1972 to 1999 for 2,309 Northern Rockies grid points versus θ [the logit(*P*)] from leave-one-out cross-validated logistic regressions of fire presence/absence on climate and topography. Shown is one example from 1,000 simulations. Fire presence was simulated with draws from binomial distributions with probability *P*, and then fire number was simulated wherever fire was present using four Poisson lognormal distributions conditional on θ.

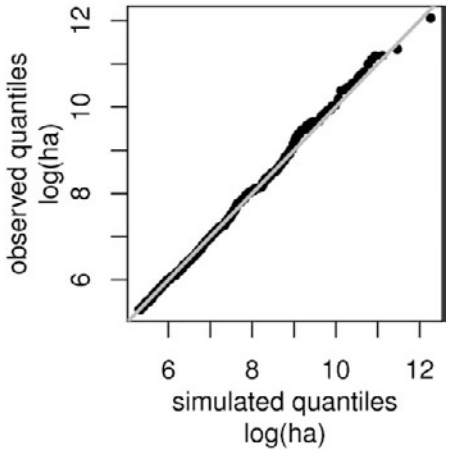

Fig. S8. Generalized Pareto distribution (GPD) fit to log(area burned) for Northern Rockies fires >200 ha observed from 1972 to 1999. Quantiles of observed versus simulated log(area burned) show the estimated GPD is a good fit to the observed data.

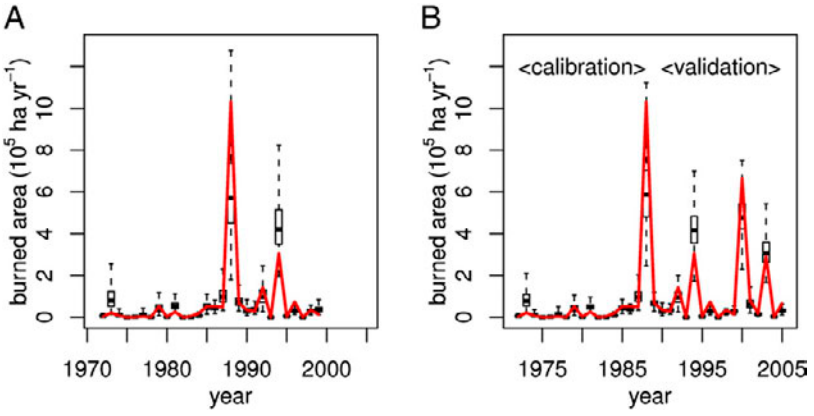

Fig. S9. (*A* and *B*) One thousand GPD simulations for historical observed fires, aggregated annually across the Northern Rockies using (*A*) 1972–1999 water–year moisture deficit derived from Maurer et al.'s (14) bias-corrected gridded climate from station observations and (*B*) 1972–1988 water–year moisture deficit derived from the NHPS gridded climate from a subset of station observations, versus observed values (red line). Simulations after 1988 (*B*, right) use GPD scale and shape parameters estimated on 1972–1988 data. Spearman rank correlation between annual mean of simulations and annual observed area burned is 0.87 for the model estimation period (1972–1988) and 0.92 for the validation period (1989–2005). (Boxes show interquartile range, and whiskers show 1.5× interquartile range).